Research Square

Preprints are preliminary reports that have not undergone peer review.
They should not be considered conclusive, used to inform clinical practice,
or referenced by the media as validated information.

Serum Gasdermin D Adds Value to FIB-4 for Identifying FAST-Defined High-Risk MASH in Patients with MASLD: A Cross-Sectional Study

Yan Zhang
Hebei Medical University
Shengqing Liu
Tianjin Medical University
Hong Zhang
Harrison International Peace Hospital
Yongning Pan
Hebei General Hospital
Xian Yu
Hebei General Hospital
Yajun Zhou
Hebei General Hospital
Guangyao Song
Hebei General Hospital
Luping Ren
renluping1122@163.com

Hebei General Hospital

Research Article

Keywords: metabolic dysfunction-associated steatotic liver disease, metabolic dysfunction-associated steatohepatitis, gasdermin D, interleukin-1β, pyroptosis

Posted Date: November 2nd, 2026

DOI: https://doi.org/10.21203/rs.3.rs-11065473/v1

License: This work is licensed under a Creative Commons Attribution 4.0 International License.
Read Full License

Additional Declarations: No competing interests reported.

Serum Gasdermin D Adds Value to FIB-4 for Identifying FAST-Defined High-Risk MASH in Patients with MASLD: A Cross-Sectional Study

Yan Zhang[1,2,3,] Shengqing Liu[4], Hong Zhang[2], Yongning Pan[3], Xian Yu[3], Yajun Zhou[3], Guangyao Song[3], Luping Ren[3,*]

1. Department of Internal Medicine, Hebei Medical University, Shijiazhuang 050000, Hebei, China
2. Department of Endocrinology, Harrison International Peace Hospital,Hengshui 053000, Hebei, China
3. Department of Endocrinology, Hebei General Hospital, Shijiazhuang 050000, Hebei, China
4. The Second Clinical Medical School, Tianjin Medical University, Tianjin 300000, China
*Correspondence: Luping Ren, Department of Endocrinology, Hebei General Hospital, Shijiazhuang 050000, Hebei, China. Email: renluping1122@163.com

Abstract

Background: Pyroptosis has been implicated in metabolic dysfunction-associated steatotic liver disease (MASLD), but the clinical relevance of circulating gasdermin D (GSDMD) remains unclear. We investigated the associations of circulating GSDMD and interleukin-1β (IL-1β) with disease severity and evaluated their incremental value for identifying FAST-defined high-risk metabolic dysfunction-associated steatohepatitis (MASH).

Methods: This cross-sectional study included 130 patients with MASLD and 70 healthy controls. Patients with MASLD were classified as having low-risk (FAST ≤ 0.35, n = 67) or high-risk MASH (FAST > 0.35, n = 63). Serum GSDMD and IL-1β concentrations were measured by enzyme-linked immunosorbent assay. Associations with high-risk MASH were evaluated using multivariable logistic regression. Discrimination and incremental performance were assessed using receiver operating characteristic curve analysis, net reclassification improvement (NRI), integrated discrimination improvement (IDI), calibration analysis, and decision curve analysis (DCA).

Results: Circulating GSDMD and IL-1β concentrations were significantly higher in patients with MASLD than in healthy controls (both $P < 0.001$), and GSDMD concentrations were higher in patients with high-risk than low-risk MASH ($P < 0.001$). Higher GSDMD concentrations were associated with greater hepatocellular injury, inflammation, and fibrosis-related abnormalities. After adjustment for age, body mass index, glycated hemoglobin, triglycerides, and FIB-4, both GSDMD (OR, 1.032; 95% CI, 1.010–1.055; $P = 0.004$) and IL-1β (OR, 1.303; 95% CI, 1.018–1.668; $P = 0.036$) remained independently associated with high-risk MASH. GSDMD alone yielded an area under the curve (AUC) of 0.785. Adding FIB-4 to clinical factors increased the AUC from 0.746 to 0.889, whereas further incorporation of GSDMD and IL-1β increased the AUC to 0.916. The integrated model improved reclassification (NRI, 1.293; IDI, 0.362; both $P < 0.001$), showed acceptable calibration, and provided greater net benefit on DCA.

Conclusions: Circulating GSDMD was associated with liver injury, inflammation, fibrosis-related abnormalities, and FAST-defined high-risk MASH. GSDMD and IL-1β provided incremental information beyond conventional clinical factors and FIB-4, supporting their potential as complementary biomarkers for non-invasive risk stratification in MASLD.

Keywords: metabolic dysfunction-associated steatotic liver disease; metabolic dysfunction-associated steatohepatitis; gasdermin D; interleukin-1β; pyroptosis

1.Background

Metabolic dysfunction-associated steatotic liver disease (MASLD) is the most prevalent chronic liver disease worldwide, affecting more than 30% of adults and imposing a substantial global health burden[1,2]. In China, its pooled prevalence is approximately 30% and is even higher among individuals with obesity, dyslipidemia, and other cardiometabolic disorders [3]. MASLD spans a broad clinical spectrum, from simple steatosis to metabolic dysfunction-associated steatohepatitis (MASH), progressive fibrosis, cirrhosis, and hepatocellular carcinoma. Because early disease is often asymptomatic, clinically relevant MASH and fibrosis may remain undetected until more advanced stages [4,5]. As lifestyle modification remains the foundation of treatment and pharmacological options for MASH

continue to expand, timely identification of patients at greatest risk has become increasingly important for clinical management [6,7].

MASLD is closely linked to systemic metabolic dysfunction. Obesity, insulin resistance, type 2 diabetes mellitus (T2DM), hypertriglyceridemia, and related cardiometabolic abnormalities contribute to both disease development and fibrosis progression [8,9]. Chronic nutrient excess and insulin resistance promote hepatic lipid accumulation and lipotoxicity, which in turn induce mitochondrial dysfunction, oxidative stress, and activation of innate immune pathways. These processes can trigger inflammasome signaling and inflammatory cell death, providing a mechanistic link between metabolic dysfunction, hepatocellular injury, and fibrogenesis [10–12]. Circulating markers of inflammatory cell death may therefore provide information that is not captured by conventional metabolic indices.

Pyroptosis is an inflammatory form of regulated cell death that has emerged as a potential mediator linking metabolic stress to hepatic inflammation and fibrosis [12–15]. Gasdermin D (GSDMD) is a key executor of canonical pyroptosis. Following inflammasome activation, inflammatory caspases cleave GSDMD to generate the active N-terminal fragment (GSDMD-N), which forms membrane pores and promotes pyroptotic cell death and the release of inflammatory mediators, including interleukin-1β (IL-1β) [13,15]. Experimental studies have shown that metabolic and lipotoxic stress activates inflammasome–caspase–GSDMD signaling, while excessive GSDMD activation aggravates hepatocellular injury and inflammatory responses. In human liver tissue, increased GSDMD and GSDMD-N expression has been observed in NASH and associated with histological activity and fibrosis [14]. These findings raise the possibility that tissue-level GSDMD activation may also be reflected in the circulation.

Liver biopsy remains the reference standard for diagnosing MASH and assessing histological activity and fibrosis, but its invasiveness, sampling variability, and limited acceptability restrict routine use [16]. Non-invasive tests therefore play a central role in clinical risk assessment. The fibrosis-4 index (FIB-4) is widely recommended as a first-line tool for identifying individuals at risk of advanced fibrosis [8], whereas the FibroScan-AST (FAST) score combines liver stiffness measurement (LSM), controlled attenuation parameter (CAP),

and aspartate aminotransferase (AST) to identify patients with steatohepatitis, significant activity, and fibrosis [9]. A FAST score of ≤0.35 is commonly used as a rule-out threshold for fibrotic MASH, with a meta-analysis of 16 studies involving 8,838 participants reporting a pooled sensitivity of 88% at this cutoff [17]. However, these tools are based largely on demographic, biochemical, and imaging-derived variables and do not directly reflect molecular inflammatory pathways such as pyroptosis. Blood-based markers of these processes may therefore provide complementary information.

Although GSDMD has been increasingly implicated in MASH pathogenesis, previous studies have largely focused on experimental models and hepatic tissue expression [18,19]. Whether circulating GSDMD reflects disease severity and improves identification of patients with higher-risk disease remains unclear. This question is particularly relevant in metabolic practice, where accessible biomarkers could help refine risk assessment in individuals with obesity, T2DM, and dyslipidemia.

We therefore examined the associations of circulating GSDMD and IL-1β with metabolic features, hepatocellular injury, inflammation, and fibrosis-related indices. We further assessed whether these biomarkers were independently associated with high-risk MASH and whether they improved discrimination beyond conventional clinical factors and FIB-4.

2.Methods

2.1 Study design and participants

This single-center, cross-sectional observational study was conducted at Hebei General Hospital between April 2025 and December 2025. The study protocol was reviewed and approved by the Institutional Review Board of Hebei General Hospital (Ethics approval number: (2025) Scientific Research Ethics Review No. 259). Participants were consecutively recruited from individuals undergoing routine health examinations with abdominal ultrasonography and from hospitalized patients with metabolic disorders. All participants underwent a standardized clinical assessment, including collection of medical history, medication use, physical examination, and anthropometric measurements. Information on

smoking, alcohol consumption, type 2 diabetes mellitus, hypertension, dyslipidemia, cardiovascular disease, thyroid disorders, gastrointestinal disorders, and use of glucose-lowering, lipid-lowering, and antihypertensive medications was recorded. Body mass index (BMI) was calculated as weight in kilograms divided by height in meters squared.

Participants were eligible for inclusion if they met the following criteria: (1) aged 18–65 years, with no restriction on sex; and (2) fulfilled the consensus-based diagnostic criteria for metabolic dysfunction-associated steatotic liver disease (MASLD). MASLD was diagnosed according to the 2023 multisociety consensus criteria and subsequent EASL–EASD–EASO clinical practice guidelines. The diagnosis required evidence of hepatic steatosis together with at least one cardiometabolic risk factor, including: (1) overweight or obesity, defined as a body mass index (BMI) ≥25 kg/m² (≥23 kg/m² in individuals of Asian ethnicity); (2) dysglycemia or type 2 diabetes mellitus, including HbA1c 5.7–6.4%, fasting plasma glucose 5.6–6.9 mmol/L, 2h plasma glucose during an oral glucose tolerance test of 7.8–11.0 mmol/L, established type 2 diabetes, or glucose-lowering treatment; (3) plasma triglycerides ≥1.7 mmol/L or lipid-lowering treatment; (4) HDL-cholesterol ≤1.0 mmol/L in men or ≤1.3 mmol/L in women, or lipid-lowering treatment; or (5) blood pressure ≥130/85 mmHg or antihypertensive treatment. Participants were excluded if they met any of the following criteria: (1) type 1 diabetes mellitus, gestational diabetes mellitus, or other specific types of diabetes; (2) acute or chronic systemic infection within 4 weeks before enrollment, severe acute diabetic complications, or acute cardiovascular or cerebrovascular events within the preceding 3 months; (3) severe hepatic or renal dysfunction, active malignancy, or systemic glucocorticoid treatment for >1 month; (4) chronic excessive alcohol consumption, defined as an average alcohol intake ≥40 g/day in men or ≥20 g/day in women for ≥5 consecutive years; (5) pregnancy or lactation; (6) chronic viral hepatitis, cirrhosis, autoimmune hepatitis, biliary tract disease, or hereditary hemochromatosis; or (7) clinically significant thyroid dysfunction requiring unstable treatment. Participants with stable subclinical thyroid dysfunction receiving unchanged replacement therapy were eligible.

After an overnight fast of 10–12 h, peripheral venous blood samples were collected in the morning. Samples were centrifuged at 3,000 rpm for 10 min at 4 °C, and serum aliquots

were immediately transferred into cryovials and stored at −80 °C until analysis. Repeated freeze–thaw cycles were avoided.

All participants underwent abdominal B-mode ultrasonography and vibration-controlled transient elastography using FibroScan® 530 (Echosens, Paris, France). Examinations were performed by trained operators blinded to laboratory biomarker results. MASLD was diagnosed according to the 2023 multisociety consensus definition, requiring evidence of hepatic steatosis together with at least one cardiometabolic risk factor. Participants were classified into a healthy control group (n = 70) and a MASLD group (n = 130). Within the MASLD cohort, participants were further stratified according to the FAST score. A FAST score ≤ 0.35 was considered low risk, whereas a FAST score > 0.35 was considered indicative of increased risk of fibrotic MASH for the purposes of the present study.

2.2 Calculation of non-invasive liver indices

FIB-4, FAST, HSI, HOMA-IR, and HOMA-β were calculated using established formulas. FIB-4 was calculated as age (years) × AST (U/L) / [platelet count (10^9/L) × √ALT (U/L)]. FAST was calculated as exp(Z)/[1 + exp(Z)], where $Z = -1.65 + 1.07 \times \ln(LSM) + 2.66 \times 10^{-8} \times CAP^3 - 63.3 \times AST^{-1}$. HSI was calculated as 8 × (ALT/AST) + BMI, with an additional 2 points each for female sex and diabetes mellitus. HOMA-IR was calculated as FBG (mmol/L) × FINS (μIU/mL) / 22.5, and HOMA-β as 20 × FINS (μIU/mL) / [FBG (mmol/L) − 3.5].

2.3 Measurement of serum GSDMD and IL-1β

Serum concentrations of gasdermin D (GSDMD) and interleukin-1β (IL-1β) were measured using commercially available human ELISA kits according to the manufacturers' instructions [GSDMD kit: Cat. No. MDTK8001, Beijing Meditech Technology Co., Ltd., Beijing, China; IL-1 β kit: Cat. No. E-EL-H0149, Elabscience Biotechnology Inc., Wuhan, China]. The assay measured total circulating GSDMD concentrations.

Frozen serum samples were thawed on ice and diluted as appropriate according to the assay protocol. Standards, blank controls, and serum samples were added to antibody-precoated 96-well plates. All samples were assayed in duplicate. After incubation

and washing, detection antibody and chromogenic substrate were added sequentially, and absorbance was measured at 450 nm using a microplate reader (VersaMax™, Molecular Devices, USA). Standard curves were generated using four-parameter logistic regression, and analyte concentrations were calculated accordingly. Assay precision was assessed using intra-assay and inter-assay coefficients of variation (CVs). Intra-assay CVs were <8%, and inter-assay CVs were <12%.

2.4 Statistical analysis

All statistical analyses were performed using SPSS version 27.0 (IBM Corp., Armonk, NY, USA) and R version 4.3.0 (R Foundation for Statistical Computing, Vienna, Austria). Normality of continuous variables was assessed using the Shapiro–Wilk test, and homogeneity of variance was evaluated using Levene's test. Normally distributed continuous variables are presented as mean ± standard deviation (SD), whereas non-normally distributed variables are expressed as median (interquartile range, IQR). Categorical variables are presented as numbers and percentages. For comparisons between two groups, an independent-samples Student's t-test was used for normally distributed variables with equal variances, whereas the Mann–Whitney U test was used otherwise. For comparisons among three groups, one-way analysis of variance was used when the assumptions of normality and homogeneity of variance were satisfied; otherwise, the Kruskal–Wallis test was applied. Correlations between continuous variables were assessed using Pearson's correlation for normally distributed data and Spearman's rank correlation for non-normally distributed or ordinal data. Univariable binary logistic regression was first performed to explore factors associated with FAST-defined high-risk MASH. Multicollinearity was assessed using variance inflation factors (VIFs), with VIF > 5 considered indicative of substantial multicollinearity. Four sequential multivariable logistic regression models were used to evaluate independent associations: Model 1 included age, body mass index (BMI), glycated hemoglobin (HbA1c), and triglycerides; Model 2 additionally included FIB-4; Model 3 comprised Model 2 plus IL-1β; and Model 4 comprised Model 3 plus GSDMD. Associations are reported as odds ratios (ORs) with 95% confidence intervals (CIs). For discrimination and incremental-performance analyses, five prespecified models were compared: Model 1

included the four clinical covariates; Model 2 added FIB-4; Model 3 added GSDMD to Model 2; Model 4 added IL-1β to Model 2; and Model 5 added both GSDMD and IL-1β to Model 2.

Receiver operating characteristic (ROC) curve analysis was used to evaluate the discriminatory performance of serum GSDMD, IL-1β, FIB-4, and the multivariable models for identifying FAST-defined high-risk MASH. The area under the ROC curve (AUC) was used as a measure of discrimination. Optimal cutoff values for individual biomarkers were determined by maximizing the Youden index, and the corresponding sensitivity, specificity, positive predictive value (PPV), and negative predictive value (NPV) were calculated. Differences in AUCs between nested models were compared using the DeLong test.

To assess the incremental value of GSDMD and IL-1β beyond conventional clinical variables and FIB-4, continuous net reclassification improvement (NRI) and integrated discrimination improvement (IDI) were calculated. Model calibration was assessed using calibration plots with 1,000 bootstrap resamples, Brier scores, calibration intercepts and slopes, and the Hosmer–Lemeshow goodness-of-fit test. Decision curve analysis (DCA) was performed to evaluate the clinical net benefit of each model across a range of threshold probabilities.

All statistical tests were two-sided, and a P value <0.05 was considered statistically significant.

3. Results

3.1 Study population and baseline characteristics

The baseline characteristics of the study population are summarized in Table 1. Compared with healthy controls, patients with MASLD exhibited a more adverse metabolic profile, greater hepatocellular injury, and increased inflammatory burden. Significant differences were observed in anthropometric measures, glycemic indices, lipid profiles, liver enzymes, CRP, CAP, liver stiffness measurement (LSM), FIB-4, HSI, and FAST score (all $P < 0.05$). Platelet count, HDL-C, ApoA1, and HOMA-β were lower in patients with MASLD, whereas age and sex distributions were comparable between groups.

Circulating GSDMD and IL-1β levels were markedly elevated in MASLD. Median serum GSDMD concentrations were 57.09 (33.18–75.04) pg/mL in patients with MASLD versus 17.29 (8.72–28.36) pg/mL in healthy controls ($P < 0.001$). Similarly, IL-1β concentrations were 2.32 (1.14–5.87) pg/mL versus 0.61 (0.31–1.11) pg/mL, respectively ($P<0.001$).

3.2 Circulating GSDMD is elevated in FAST-defined high-risk MASH

Within the MASLD cohort, 67 patients were classified as low risk (FAST ≤0.35) and 63 as high risk (FAST >0.35). Serum GSDMD and IL-1β concentrations were significantly higher in the FAST-defined high-risk group than in the low-risk group (both $P<0.001$; Figure 1 a, b).

Stratified analyses by sex, BMI, and FIB-4 category showed a consistent pattern, with higher circulating GSDMD concentrations in patients with FAST-defined high-risk MASH across the examined subgroups (both $P < 0.001$; Figure 2 a – e). These findings indicate that the association between circulating GSDMD and FAST-defined disease severity was not confined to a single demographic or fibrosis-risk stratum.

3.3 Clinical characteristics across serum GSDMD tertiles

Patients with MASLD were categorized into tertiles according to circulating GSDMD concentrations. Increasing GSDMD tertiles were accompanied by progressively higher ALT, AST, GGT, triglycerides, CRP, IL-1β, LSM, and FIB-4 levels and lower HDL-C concentrations (all $P<0.05$; Table 2).

In contrast, BMI, blood pressure, glucose metabolism-related indices, and CAP did not differ significantly across GSDMD tertiles. Thus, the gradient in circulating GSDMD was more closely aligned with hepatocellular injury, inflammation, and fibrosis-related abnormalities than with the degree of hepatic steatosis assessed by CAP.

3.4 Correlations of GSDMD and IL-1β with disease severity

Correlation analysis demonstrated that circulating GSDMD and IL-1β were positively associated with FAST score and with biochemical or non-invasive indices reflecting

hepatocellular injury, inflammation, and fibrosis. FAST score showed significant positive correlations with GSDMD (r=0.503, P<0.001), IL-1β (r=0.468, P<0.001), FIB-4 (r=0.515, P<0.001), LSM (r=0.544, P<0.001), ALT (r=0.759, P<0.001), AST (r=0.950, P<0.001), GGT (r=0.471, P<0.001), triglycerides (r=0.380, P<0.001), and CRP (r=0.302, P<0.001). An inverse correlation was observed between FAST and HDL-C (r=−0.418, P<0.001).(Table 3, Figure 3)

These findings support a close relationship between pyroptosis-related biomarkers and the inflammatory and fibrosis-related components of MASLD severity.

3.5 Factors independently associated with FAST-defined high-risk MASH

In univariable logistic regression analyses, multiple clinical and biochemical variables were associated with FAST-defined high-risk MASH. FIB-4 showed a strong association (OR, 7.906; 95% CI, 3.209–19.481; P < 0.001). Circulating GSDMD (OR, 1.041; 95% CI, 1.024–1.057; P<0.001) and IL-1β (OR, 1.350; 95% CI, 1.177–1.547; P<0.001) were also significantly associated with high-risk MASH (Table 4)

Multicollinearity was assessed before multivariable modeling. VIF values ranged from 1.082 to 1.843 for the variables included in the final models, indicating no substantial multicollinearity.(Table 5)

After adjustment for age, BMI, HbA1c, triglycerides, and FIB-4, both GSDMD and IL-1β remained independently associated with FAST-defined high-risk MASH. For GSDMD, the adjusted OR was 1.032 (95% CI, 1.010–1.055; P=0.004), corresponding to a 3.2% increase in the odds of high-risk MASH per 1-pg/mL increase in circulating GSDMD. IL-1β was also independently associated with high-risk MASH (OR, 1.303; 95% CI, 1.018–1.668; P=0.036). FIB-4 remained strongly associated with high-risk MASH (OR, 16.560; 95% CI, 4.170–65.771; P < 0.001) (Table 6)

3.6 Discriminatory performance of individual biomarkers

ROC curve analyses were performed to compare the ability of individual biomarkers to discriminate FAST-defined high-risk MASH. Among the single markers, GSDMD showed

the highest AUC at 0.785 (95% CI, 0.702–0.867), followed by FIB-4 at 0.768 (95% CI, 0.685–0.850) and IL-1β at 0.747 (95% CI, 0.663–0.831).

At an optimal cutoff of 52.88 pg/mL, GSDMD yielded a sensitivity of 85.7%, specificity of 71.6%, positive predictive value of 74.0%, negative predictive value of 84.2%, and a Youden index of 0.573. The corresponding Youden indices for FIB-4 and IL-1β were 0.458 and 0.387, respectively (Table 7, Figure 4)

3.7 Incremental value of GSDMD and IL-1β beyond clinical factors and FIB-4

Five sequential models were constructed to evaluate the incremental discriminatory value of GSDMD and IL-1β. The clinical model (Model 1) showed moderate discrimination, with an AUC of 0.746 (95% CI, 0.661–0.831). Adding FIB-4 (Model 2) increased the AUC to 0.889 (95% CI, 0.837–0.942; ΔAUC, 0.143; DeLong P<0.001).

Further addition of GSDMD (Model 3) increased the AUC to 0.913 (95% CI, 0.866–0.959), whereas addition of IL-1β (Model 4) yielded an AUC of 0.905 (95% CI, 0.856–0.953). The fully integrated model incorporating both GSDMD and IL-1β (Model 5) achieved the highest discrimination, with an AUC of 0.916 (95% CI, 0.870–0.961; ΔAUC vs Model 1, 0.170; DeLong P<0.001).(Table 8, Figure 5)

Continuous NRI and IDI analyses further demonstrated incremental improvement in risk classification. Compared with Model 1, Model 5 yielded an NRI of 1.2926 (95% CI, 1.0301–1.5550; P<0.001) and an IDI of 0.3622 (95% CI, 0.2780–0.4465; P<0.001), representing the greatest reclassification improvement among the five models.(Table 9)

3.8 Calibration of the prediction models

Internal calibration was assessed using 1,000 bootstrap resamples. Brier scores decreased from 0.204 in Model 1 to 0.115 in Model 5, indicating improved overall prediction error with progressive model refinement. The calibration intercepts remained close to zero across all models (−0.007 to −0.038), whereas calibration slopes ranged from 0.799 to 0.866.

The Hosmer–Lemeshow goodness-of-fit test was non-significant for all models (Model 1, P=0.115; Model 2, P=0.178; Model 3, P=0.645; Model 4, P=0.375; Model 5, P=0.776).

The fully integrated model showed a Brier score of 0.115, calibration intercept of −0.038, calibration slope of 0.799, and Hosmer–Lemeshow P value of 0.776, indicating acceptable agreement between predicted and observed probabilities. (Table 10)

3.9 Clinical utility of the prediction models

Decision curve analysis demonstrated that models incorporating FIB-4 and the pyroptosis-related biomarkers generally provided greater net benefit than the clinical model alone across a broad range of threshold probabilities(Fig. 6). Models 3–5 maintained favorable net benefit across much of the clinically relevant threshold range, whereas Model 1 showed a more limited net benefit as the threshold probability increased.

The fully integrated model incorporating FIB-4, GSDMD, and IL-1β showed an overall favorable clinical net benefit, supporting the potential value of adding pyroptosis-related biomarkers to conventional clinical risk assessment for identifying patients with FAST-defined high-risk MASH.

4. Discussion

In this study, circulating GSDMD and IL-1β levels were significantly elevated in MASLD and were associated with a higher likelihood of high-risk MASH as defined by FAST. Higher GSDMD concentrations were accompanied by greater hepatocellular injury, systemic inflammation, and fibrosis-related abnormalities, whereas CAP did not differ significantly across GSDMD tertiles. After adjustment for age, BMI, HbA1c, triglycerides, and FIB-4, both GSDMD and IL-1β remained independently associated with high-risk disease. Adding these pyroptosis-related biomarkers to a model containing conventional clinical factors and FIB-4 improved discrimination and reclassification, with the fully integrated model achieving the highest AUC. These findings support the potential value of circulating GSDMD as an adjunctive marker for risk stratification in MASLD.

MASLD is increasingly recognized as a systemic metabolic disorder rather than an isolated consequence of hepatic fat accumulation. Obesity, insulin resistance, type 2 diabetes mellitus (T2DM), dyslipidemia, and chronic metabolic inflammation are closely linked to both disease development and progression [3,5,20]. Chronic nutrient excess and insulin

resistance increase hepatic lipid flux and lipotoxic stress, leading to mitochondrial dysfunction, oxidative stress, and activation of innate immune pathways [11,21,22]. These processes can promote inflammasome activation and inflammatory cell death, thereby linking metabolic dysfunction to hepatocellular injury and fibrogenesis [18,23]. This concept is consistent with our observation that MASLD was accompanied by higher HbA1c, adverse lipid profiles, and a greater inflammatory burden than in healthy controls. Moreover, increasing GSDMD tertiles were associated with progressive elevations in ALT, AST, GGT, CRP, LSM, and FIB-4, whereas CAP remained unchanged. This pattern suggests that circulating GSDMD may be more closely related to inflammatory and fibrotic activity than to hepatic fat accumulation per se.

Pyroptosis has emerged as an important mechanism linking metabolic stress to hepatic inflammation and fibrosis [18]. As a highly inflammatory form of regulated cell death, it has been implicated in infectious [24,25], metabolic [26,27], cardiovascular [28], neurodegenerative [29], and malignant diseases [30]. Activation of the NLRP3 inflammasome promotes caspase-1 activation, followed by GSDMD cleavage and maturation of pro-inflammatory cytokines such as IL-1β and IL-18. The N-terminal fragment of GSDMD forms membrane pores and acts as a key executor of pyroptotic cell death [31–34]. Evidence from both human and experimental studies supports the involvement of inflammasome–pyroptosis signaling in steatohepatitis. Hepatic NLRP3-related signaling is enhanced in NASH and has been linked to fibrogenic responses [35]. Xu et al. [18] further showed that hepatic GSDMD-N expression was increased in NASH and correlated with histological activity and fibrosis, whereas GSDMD deficiency attenuated experimental steatohepatitis. More recently, IRE1α, NLRP3, and GSDMD/GSDMD-N were reported to be upregulated in human MASH liver, while pharmacological or genetic inhibition of IRE1α suppressed pyroptosis and ameliorated experimental disease [19]. Circulating GSDMD should not be interpreted as a direct surrogate of hepatic GSDMD activation alone. Instead, it may represent a systemic indicator of pyroptosis-related inflammatory activity, integrating signals derived from hepatocytes, hepatic immune cells, and other metabolically active tissues [36,37]. Previous studies have demonstrated that GSDMD-mediated pyroptosis occurs across multiple cell types, including

hepatocytes and immune cells, and contributes to inflammatory amplification through IL-1β/IL-18 release [38,39].

The interaction between metabolic dysfunction and pyroptosis may be especially relevant in individuals with T2DM, obesity, and dyslipidemia. Insulin resistance and nutrient excess can promote lipotoxicity, oxidative stress, and inflammasome activation, while inflammasome-derived cytokines may in turn aggravate metabolic inflammation and insulin resistance [21,40,41]. Such bidirectional interactions may contribute to disease progression. Nevertheless, the cross-sectional design precludes conclusions regarding whether diabetes or dyslipidemia directly contributes to elevated circulating GSDMD. Studies across different metabolic phenotypes and treatment backgrounds will be needed to clarify these relationships.

The distinct biological roles of GSDMD and IL-1β may partly explain their different discriminatory performance. IL-1β is a downstream inflammasome-related cytokine that reflects inflammatory signaling, whereas GSDMD directly executes canonical pyroptosis through membrane pore formation and release of inflammatory mediators [25,26]. In our cohort, IL-1β remained independently associated with high-risk MASH but showed a less consistent gradient across GSDMD tertiles, while GSDMD had the highest AUC among the individual biomarkers. These findings are compatible with their different positions within the pyroptotic cascade. IL-1β nevertheless remains relevant to fibrogenesis because it can amplify hepatic inflammation and promote hepatic stellate cell activation and profibrotic responses [42]. GSDMD and IL-1β may therefore provide complementary rather than redundant information: the former may more closely reflect pyroptotic execution, whereas the latter represents downstream inflammatory signaling. Their combined assessment may capture a broader component of the pyroptosis–inflammation axis, consistent with the improved discrimination and reclassification observed in the integrated model.

Our findings should be interpreted in the context of established non-invasive approaches for MASLD risk stratification. FIB-4 is widely recommended as a first-line fibrosis assessment tool; however, it primarily reflects fibrosis risk and does not capture inflammatory activity. The FAST score, developed by Newsome et al. [9], integrates liver stiffness

measurement, controlled attenuation parameter, and AST to identify patients with steatohepatitis and significant fibrosis risk. A cutoff value of 0.35 was proposed as a sensitive threshold to exclude individuals with at-risk NASH in the original derivation and validation cohorts. Therefore, FAST provides a practical and non-invasive endpoint that minimizes the limitations of liver biopsy, including invasiveness and sampling variability. Nevertheless, FAST remains a surrogate marker of histological disease activity and cannot determine individual NAS components or fibrosis stage. Thus, our findings cannot establish whether circulating GSDMD is specifically associated with lobular inflammation, hepatocyte ballooning, or fibrosis severity, highlighting the need for histological validation.

Among the individual biomarkers evaluated, GSDMD demonstrated the highest AUC, although its numerical superiority over FIB-4 should not be interpreted as statistical dominance without formal pairwise comparison. Importantly, incorporation of GSDMD and IL-1β into the FIB-4-based clinical model significantly improved discrimination, with the combined model achieving an AUC of 0.916 and showing enhanced reclassification performance based on NRI and IDI. These findings suggest that pyroptosis-related biomarkers provide complementary information beyond conventional metabolic risk factors and fibrosis-oriented parameters.

The incremental value of GSDMD may be particularly relevant in metabolic and endocrine settings, where obesity, type 2 diabetes, and dyslipidemia frequently coexist with MASLD progression [5,17]. As a circulating biomarker, GSDMD may complement routine metabolic evaluation and FIB-4 assessment to identify individuals who require further FibroScan evaluation or specialist referral. It may also improve risk stratification among patients with indeterminate results from conventional non-invasive tests. However, GSDMD should be considered an adjunctive biomarker rather than a replacement for established clinical algorithms.

Several limitations should be acknowledged. First, the single-center cross-sectional design prevents causal inference and limits evaluation of the longitudinal prognostic value of circulating GSDMD and IL-1β. Second, high-risk MASH was defined using FAST rather than liver biopsy; therefore, associations with specific histological features, including NAS

components, inflammatory activity, and fibrosis stage, could not be directly assessed. Third, we measured circulating GSDMD and IL-1β but did not evaluate hepatic expression of key components within the NLRP3/caspase-1/GSDMD pathway, limiting mechanistic interpretation. Fourth, potential effects of metabolic therapies, including glucose-lowering, lipid-lowering, and weight-loss interventions, on circulating GSDMD levels were not fully evaluated. Finally, the relatively modest sample size and absence of external validation may affect model robustness and generalizability. Future multicenter prospective studies incorporating histological validation, longitudinal biomarker assessment, and external validation cohorts are warranted.

5. Conclusions

Circulating GSDMD was independently associated with FAST-defined high-risk MASH in patients with MASLD and provided complementary information beyond conventional clinical factors and FIB-4. Incorporating GSDMD and IL-1β into a FIB-4-based clinical model improved discrimination, reclassification, and clinical net benefit. These findings support further evaluation of circulating GSDMD as an adjunctive biomarker for non-invasive MASLD risk stratification. Prospective multicenter studies with histological and external validation are warranted.

Declarations

Ethics approval and consent to participate

The study protocol was reviewed and approved by the Institutional Review Board of Hebei General Hospital (approval no. (2025) Scientific Research Ethics Review No. 259) and was conducted in accordance with the Declaration of Helsinki and its subsequent amendments. Informed consent was obtained from all participants before enrollment. Written informed consent was obtained from all participants before enrollment.

Consent for publication

Not applicable.

Clinical trial number

Not applicable.

Availability of data and materials

The datasets generated and/or analyzed during the current study are available from the corresponding author on reasonable request.

Competing interests

The authors declare that they have no competing interests.

Funding

This work was supported by the Natural Science Foundation of Hebei Province (Grant No. H2025307007), the Hebei Provincial Medical Science Research Project (Grant No. GZ20260147), and the Hebei Provincial Medical Science Research Program (Grant No. 20230011).

Authors' contributions

LP-R: Conceptualization, Methodology, Supervision, Validation, Funding acquisition,Project administration, Writing – review & editing. YZ: Conceptualization, Data curation, Formal Analysis, Validation, Writing – original draft, Writing – review & editing. SQ-L: Writing – original draft, Data curation, Methodology, Resources, Validation. HZ: Conceptualization, Writing – original draft, Data curation, Resources, Validation. YN-P: Writing – original draft, Data curation, Formal Analysis, Project administration, Investigation, Validation. XY:Formal Analysis, Project administration. YJ-Z:Project administration, Investigation, Validation. GY-S:Methodology, Supervision, Validation, Writing – review & editing, Funding acquisition, Project administration.All authors read and approved the final manuscript.

Acknowledgements

Not applicable.

References

[1] Younossi ZM, Golabi P, Paik JM, Henry A, Van Dongen C, Henry L. The global epidemiology of nonalcoholic fatty liver disease (NAFLD) and nonalcoholic

steatohepatitis (NASH): a systematic review. Hepatology. 2023;77(4):1335-1347. doi:10.1097/HEP.0000000000000004.

[2] Rinella ME, Lazarus JV, Ratziu V, Francque SM, Sanyal AJ, Kanwal F, et al. A multisociety Delphi consensus statement on new fatty liver disease nomenclature. J Hepatol. 2023;79(6):1542-1556. doi:10.1016/j.jhep.2023.06.003.

[3] Loomba R, Friedman SL, Shulman GI. Mechanisms and disease consequences of nonalcoholic fatty liver disease. Cell. 2021;184(10):2537-2564. doi:10.1016/j.cell.2021.04.015.

[4] Powell EE, Wong VW-S, Rinella M. Non-alcoholic fatty liver disease. Lancet. 2021;397(10290):2212-2224. doi:10.1016/S0140-6736(20)32511-3.

[5] European Association for the Study of the Liver (EASL); European Association for the Study of Diabetes (EASD); European Association for the Study of Obesity (EASO). EASL-EASD-EASO Clinical Practice Guidelines on the management of metabolic dysfunction-associated steatotic liver disease (MASLD). J Hepatol. 2024;81(3):492-542. doi:10.1016/j.jhep.2024.04.031.

[6] Tincopa MA, Anstee QM, Loomba R. New and emerging treatments for metabolic dysfunction-associated steatohepatitis. Cell Metab. 2024;36(5):912-926. doi:10.1016/j.cmet.2024.03.011.

[7] Kleiner DE, Brunt EM, Van Natta M, Behling C, Contos MJ, Cummings OW, et al. Design and validation of a histological scoring system for nonalcoholic fatty liver disease. Hepatology. 2005;41(6):1313-1321. doi:10.1002/hep.20701.

[8] Sterling RK, Lissen E, Clumeck N, Sola R, Correa MC, Montaner J, et al. Development of a simple noninvasive index to predict significant fibrosis in patients with HIV/HCV coinfection. Hepatology. 2006;43(6):1317-1325. doi:10.1002/hep.21178.

[9] Newsome PN, Sasso M, Deeks JJ, Paredes A, Boursier J, Chan WK, et al. FibroScan-AST (FAST) score for the non-invasive identification of patients with non-alcoholic steatohepatitis with significant activity and fibrosis: a prospective

505 derivation and global validation study. Lancet Gastroenterol Hepatol. 2020;5(4):362-373.
506 doi:10.1016/S2468-1253(19)30383-8.

507 [10] Buzzetti E, Pinzani M, Tsochatzis EA. The multiple-hit pathogenesis of non-alcoholic
508 fatty liver disease (NAFLD). Metabolism. 2016;65(8):1038-1048.
509 doi:10.1016/j.metabol.2015.12.012.

510 [11] Friedman SL, Neuschwander-Tetri BA, Rinella M, Sanyal AJ. Mechanisms of NAFLD
511 development and therapeutic strategies. Nat Med. 2018;24(7):908-922.
512 doi:10.1038/s41591-018-0104-9.

513 [12] Shi J, Zhao Y, Wang K, Shi X, Wang Y, Huang H, et al. Cleavage of GSDMD by
514 inflammatory caspases determines pyroptotic cell death. Nature.
515 2015;526(7575):660-665. doi:10.1038/nature15541.

516 [13] Stoess C, Leszczynska A, Kui L, Feldstein AE. Pyroptosis and gasdermins— Emerging
517 insights and therapeutic opportunities in metabolic dysfunction-associated steatohepatitis.
518 Front Cell Dev Biol. 2023;11:1218807. doi:10.3389/fcell.2023.1218807.

519 [14] Mridha AR, Wree A, Robertson AAB, Yeh MM, Johnson CD, Van Rooyen DM, et al.
520 NLRP3 inflammasome blockade reduces liver inflammation and fibrosis in experimental
521 NASH in mice. J Hepatol. 2017;66(5):1037-1046. doi:10.1016/j.jhep.2017.01.022.

522 [15] Liu X, Zhang Z, Ruan J, Pan Y, Magupalli VG, Wu H, et al. Inflammasome-activated
523 gasdermin D causes pyroptosis by forming membrane pores. Nature. 2016;535(7610):
524 153-158. doi:10.1038/nature18629.

525 [16] Ipsen DH, Lykkesfeldt J, Tveden-Nyborg P. Molecular mechanisms of hepatic lipid
526 accumulation in non-alcoholic fatty liver disease. Cell Mol Life Sci.
527 2018;75(18):3313-3327. doi:10.1007/s00018-018-2860-6.

528 [17] Malandris K, Arampidis D, Mainou M, Papadopoulos N, Karagiannis T, Nayfeh T, et al.
529 FibroScan-AST score for diagnosing fibrotic MASH: a systematic review and
530 meta-analysis of diagnostic test accuracy studies. J Gastroenterol Hepatol.
531 2024;39(12):2582-2591. doi:10.1111/jgh.16770.

[18] Xu B, Jiang M, Chu Y, Wang W, Chen D, Li X, et al. Gasdermin D plays a key role as a pyroptosis executor of non-alcoholic steatohepatitis in humans and mice. J Hepatol. 2018;68(4):773-782. doi:10.1016/j.jhep.2017.11.040.

[19] Zeng X, Wu T, Xu Q, Li L, Yuan Y, Zhu M, et al. Inhibition of IRE-1α alleviates pyroptosis and metabolic dysfunction-associated steatohepatitis by suppressing gasdermin D. Liver Int. 2025;45(2):e16234. doi:10.1111/liv.16234.

[20] Cariou B, Byrne CD, Loomba R, Sanyal AJ. Nonalcoholic fatty liver disease as a metabolic disease in humans: a literature review. Diabetes Obes Metab. 2021;23(5):1069-1083. doi:10.1111/dom.14322.

[21] Bansal SK, Bansal MB. Pathogenesis of MASLD and MASH—role of insulin resistance and lipotoxicity. Aliment Pharmacol Ther. 2024;59(Suppl 1):S10-S22. doi:10.1111/apt.17930.

[22] Li Y, Yang P, Ye J, Xu Q, Wu J, Wang Y, et al. Updated mechanisms of MASLD pathogenesis. Lipids Health Dis. 2024;23:117. doi:10.1186/s12944-024-02108-x.

[23] Zheng D, Liwinski T, Elinav E.Inflammasome activation and regulation: toward a better understanding of complex mechanisms.Cell Discov. 2020;6:36. doi:10.1038/s41421-020-0167-x.

[24] Kelley N, Jeltema D, Duan Y, He Y. The NLRP3 inflammasome: an overview of mechanisms of activation and regulation.Int J Mol Sci. 2019;20(13):3328. doi:10.3390/ijms20133328.

[25] He WT, Wan H, Hu L, Chen P, Wang X, Huang Z, et al. Gasdermin D is an executor of pyroptosis and required for interleukin-1β secretion. Cell Res. 2015;25(12):1285-1298. doi:10.1038/cr.2015.139.

[26] Tilg H, Moschen AR, Roden M.NAFLD and diabetes mellitus.Nat Rev Gastroenterol Hepatol. 2017;14(1):32-42. doi:10.1038/nrgastro.2016.147.

[27] Sanyal AJ, Van Natta ML, Clark J, Neuschwander-Tetri BA, Diehl AM, Dasarathy S, et al. Prospective study of outcomes in adults with nonalcoholic fatty liver disease N Engl J Med. 2021;385(17):1555-1564. doi:10.1056/NEJMoa2029349.

[28] Weng Y, Ye B, Lin J, Lin S, Zhong L, Huang W, et al. Elevated circulating levels of gasdermin D are related to acute myocardial infarction and pyroptosis. BMC Cardiovasc Disord. 2022;22(1):554. doi:10.1186/s12872-022-02998-8.

[29] Frank D, Vince JE. Pyroptosis versus necroptosis: similarities, differences, and crosstalk. Cell Death Differ. 2019;26(1):99-114.

[30] Broz P, Pelegrín P, Shao F. The gasdermins, a protein family executing cell death and inflammation. Nat Rev Immunol. 2020;20(3):143–157. doi:10.1038/s41577-019-0228-2.

[31] Jorgensen I, Miao EA. Pyroptotic cell death defends against intracellular pathogens. Immunol Rev. 2015;265(1):130-142. doi:10.1111/imr.12287.

[32] Vande Walle L, Lamkanfi M. Pyroptosis. Curr Biol. 2016;26(13):R568-R572.

[33] McKenzie BA, Mamik MK, Saito LB, Boghozian R, Monaco MC, Major EO, et al. Caspase-1 inhibition prevents glial inflammasome activation and pyroptosis in models of multiple sclerosis. Proc Natl Acad Sci U S A. 2018;115(3):E606-E615. doi:10.1073/pnas.1722041115.

[34] Shi J, Zhao Y, Wang K, Shi X, Wang Y, Huang H, et al. Cleavage of GSDMD by inflammatory caspases determines pyroptotic cell death. Nature. 2015;526(7575):660-665. doi:10.1038/nature15541.

[35] Wree A, McGeough MD, Peña CA, Schlattjan M, Li H, Inzaugarat ME, et al. NLRP3 inflammasome activation is required for fibrosis development in NAFLD. J Mol Med (Berl). 2014;92(10):1069-1082. doi:10.1007/s00109-014-1170-1.

[36] Zhu C, Li X, Wang Y, Zhang Y, Wang X, Liu Y, et al. The gasdermin family: emerging therapeutic targets in diseases. Signal Transduct Target Ther. 2024;9:105. doi:10.1038/s41392-024-01801-8.

[37] Yang S, Zhang Y, Wang Y, Li X, Chen H.Dual role of pyroptosis in liver diseases.

584 Cell Death Dis. 2025;16:105. doi:10.1038/s41419-025-07431-6.

585 [38] Broz P. Pyroptosis: molecular mechanisms and roles in disease.Nat Rev Immunol.
586 2025;25:1-17.

587 [39] Li R, Chen X, Zhang Y, Li J. Research progress of pyroptosis in fatty liver disease. Int J
588 Mol Sci. 2023;24(17):13065.doi:10.3390/ijms241713065.

589 [40] Hammerich L, Tacke F. Hepatic inflammatory responses in liver fibrosis. Nat Rev
590 Gastroenterol Hepatol. 2023;20(10):633-646. doi:10.1038/s41575-023-00807-x.

591 [41] Robert S, Gicquel T, Bodin A, Lagente V, Boichot E. Characterization of the MMP/TIMP
592 imbalance and collagen production induced by IL-1β or TNF-α release from human
593 hepatic stellate cells. PLoS One. 2016;11(4):e0153118.
594 doi:10.1371/journal.pone.0153118.

595 [42] Zhang YP, Yao XX, Zhao X. Role of c-Jun N-terminal kinase and p38/activation
596 protein-1 in interleukin-1β-mediated type I collagen synthesis in rat hepatic stellate cells.
597 APMIS. 2012;120(2):101-107. doi:10.1111/j.1600-0463.2011.02816.x.

598

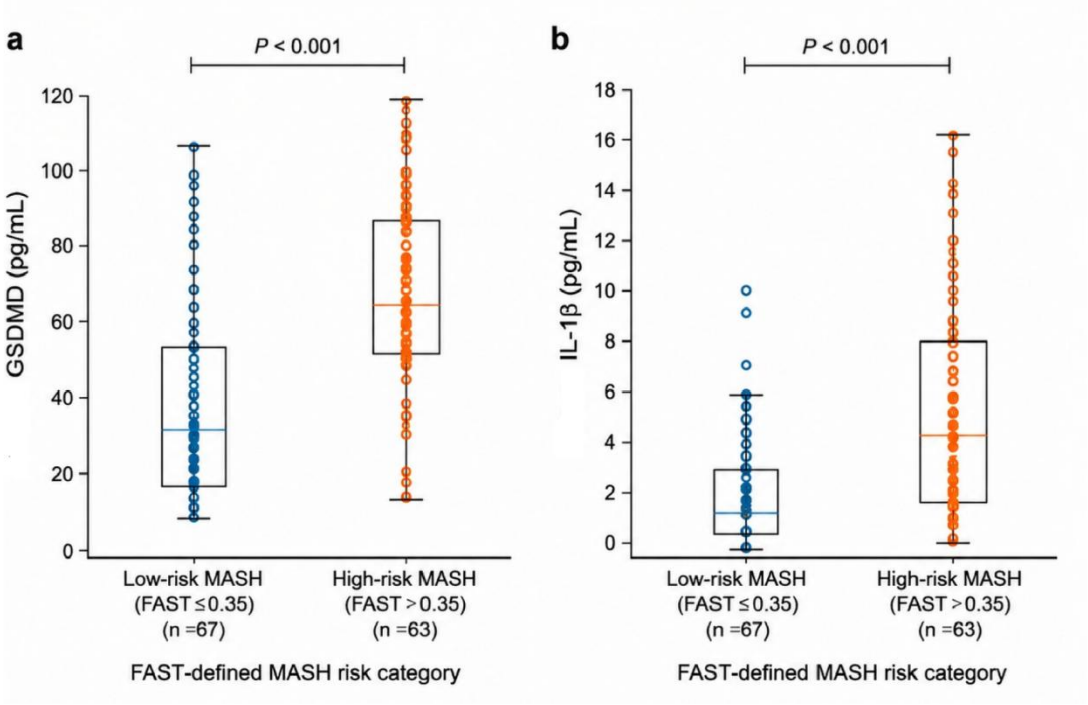
599 **Table 1. Baseline characteristics of study participants**

	Healthy control group (N=70)	**MASLD (N=130)**	**P**
Age	51(46,57)	50(43,57)	0.553
Male, n (%)	37(52.9)	69(53.1)	0.96
WC(cm)	78.33±7.13	99.72±11.28	<0.001
HC (cm)	95.03±6.06	104.49±8.58	<0.001
BMI（$kg/m^{2)}$	22.3±2.08	29.73±3.31	<0.001
SBP(mmHg)	120.73 ± 13.46	128.02±14.56	0.001
DBP (mmHg)	76.61±8.95	86.81±9.86	<0.001
PLT($\times 10^9$/L)	236.41±34.07	220.36±53.28	0.01
RDW-SD (fL)	41.63±2.03	40.48±2.7	0.001
MPV (fl)	9.98±0.65	10.86±1.28	<0.001
HbA1c (%)	5.44±0.3	8.71±1.95	<0.001
ALT (U/L)	18(14.8,22.4)	32.6(20,70)	<0.001
AST (U/L)	17.1 (15,19.9)	30.5 (20.9,55.7)	<0.001
TBIL (μmol/L)	14.27±4.29	14.33±4.45	0.93

	Healthy control group (N=70)	MASLD (N=130)	P
GGT (U/L)	15.9 (13,20.6)	41.65 (28,60.2)	<0.001
ALP (U/L)	77.55 (62.8,91)	77.95 (65,96.9)	0.259
TC (mmol/L)	4.43±0.58	5.05±1.02	<0.001
TG (mmol/L)	0.86 (0.65,1.23)	2.03 (1.49,2.99)	<0.001
HDL-C (mmol/L)	1.52±0.29	1.05±0.24	<0.001
LDL-C (mmol/L)	2.56±0.53	2.77±0.84	0.031
VLDL-C (mmol/L)	0.65(0.54,0.77)	1.24 (0.84,1.73)	<0.001
ApoA1(g/L)	1.42±0.2	1.3±0.25	<0.001
ApoB(g/L)	0.93±0.15	1.06±0.25	<0.001
UA(μmol/L)	302.75±66.38	355.37±93.34	<0.001
FBG (mmol/L)	5.28±0.37	8.11±1.79	<0.001
FINS (uU/ml)	13.96 (11.83,17.69)	13.6 (8.57,23.43)	0.392
CRP (mg/L)	0.55 (0.39,0.76)	3.01 (1.89,4.51)	<0.001
GSDMD (pg/ml)	17.29 (8.72, 28.36)	57.09(33.18,75.04)	<0.001
IL-1β (pg/ml)	0.61(0.31,1.11)	2.32(1.14,5.87)	<0.001
CAP	214.5(178,235)	308.5(287,334)	0.001
LSM (kPa)	4.05(3.4,4.7)	6.7(5.8,7.9)	<0.001
HOMA-β	169.72 (120.08, 229.37)	68.61(44.57,97.89)	<0.001
HOMA-IR	3.39(2.77,4.24)	5.49(2.77,8.58)	0.001
FIB-4	0.85(0.76,0.97)	1.22(0.97,1.69)	<0.001
HSI	30.35(28.48,32.15)	39.51(37.97,42.94)	<0.001
FAST	0.026(0.014,0.048)	0.31(0.11,0.52)	<0.001

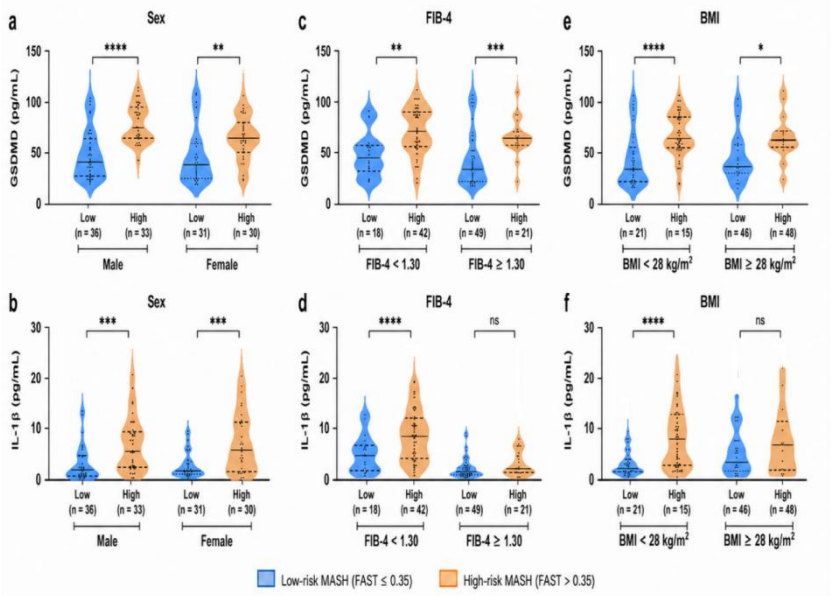
Data are presented as mean ± SD, median (IQR), or n (%), as appropriate. P values are from between-group comparisons. SD, standard deviation; IQR, interquartile range; MASLD, metabolic dysfunction-associated steatotic liver disease.

Figure 1. Circulating GSDMD and IL-1β by FAST-defined MASH risk category. Patients with MASLD were stratified into low-risk (FAST ≤ 0.35, n = 67) and high-risk (FAST > 0.35, n = 63) groups. (a) Serum GSDMD concentrations. (b) Serum IL-1β concentrations. Each point represents one participant; boxes show the median and interquartile range. P values are shown in the figure. GSDMD, gasdermin D; IL-1β, interleukin-1β; FAST, FibroScan-AST score; MASH, metabolic dysfunction-associated steatohepatitis; MASLD, metabolic dysfunction-associated steatotic liver disease.



610

611 **Figure 2.** Subgroup analyses of GSDMD and IL-1β by FAST-defined MASH risk category. Serum GSDMD (a, c,
612 e) and IL-1β (b, d, f) concentrations were compared between low-risk (FAST ≤ 0.35) and high-risk (FAST > 0.35)
613 groups after stratification by sex (a, b), FIB-4 category (c, d), and BMI category (e, f). Each point represents one
614 participant. Statistical significance is indicated within the figure. BMI, body mass index; FIB-4, fibrosis-4 index;
615 GSDMD, gasdermin D; IL-1β, interleukin-1β; FAST, FibroScan-AST score; MASH, metabolic
616 dysfunction-associated steatohepatitis.



617 **Table 2. Clinical characteristics across serum GSDMD tertiles**

Variable	GSDMD tertile 1 (n=44)	GSDMD tertile 2 (n=43)	GSDMD tertile 3 (n=43)	Statistical value, p	p1, p2, p3
Age	52.39±7.56	49.56±7.62	48.21±8.42	3.197,0.044	0.219,0.039,0.707
Male, n (%)	20 (45.5%)	23 (53.5%)	26 (60.5%)	1.972,0.373	0.593,0.235,0.663
Smoking, n (%)	6 (13.6%)	6 (14.0%)	7 (16.3%)	0.144,0.93	1,0.964,1
Alcohol, n (%)	3 (6.8%)	3 (7.0%)	6 (14.0%)	1.711,0.425	1,0.459,0.481
Hypertension, n (%)	15 (34.1%)	17 (39.5%)	14 (32.6%)	0.506,0.776	0.761,1,0.653
Diabetes mellitus, n (%)	32 (72.7%)	35 (81.4%)	34 (79.1%)	1.013,0.603	0.651,0.412,1
CVD, n (%)	4 (9.1%)	5 (11.6%)	5 (11.6%)	0.195,0.907	0.971,0.971,1
CeVD, n (%)	10 (22.7%)	6 (14.0%)	6 (14.0%)	1.594,0.451	0.436,0.436,1
Statin use, n (%)	14 (31.8%)	11 (25.6%)	6 (14.0%)	3.928,0.14	0.685,0.084,0.279
WC (cm)	97.73±11.48	101.54±11.94	99.93±10.29	1.255,0.289	0.259,0.634,0.787
HC (cm)	103.02±7.87	106.54±9.75	103.93±7.81	1.986,0.142	0.136,0.873,0.335
BMI（$kg/m^{2)}$	29.63±3.26	29.93±3.71	29.63±2.98	0.119,0.888	0.907,1,0.906
SBP (mmHg)	127.25±14.75	128.4±14.5	128.42±14.75	0.091,0.913	0.93,0.927,1.000
DBP (mmHg)	85.66±9.69	87.19±9.88	87.6±10.14	0.467,0.628	0.753,0.631,0.979
PLT($\times 10^9$/L)	219.84±42.17	226.74±59	214.51±57.79	0.566,0.569	0.819,0.888,0.54
RDW-SD (fL)	40.78±3.12	39.93±2.13	40.72±2.71	1.651,0.198	0.368,1.000,0.351
MPV (fl)	10.6±1.04	10.9±1.48	11.09±1.27	1.68,0.191	0.511,0.168,0.762
HbA1c (%)	8.23±1.74	8.78±2.03	9.11±2.03	2.282,0.106	0.391,0.091,0.706
ALT (U/L)	22.6 (16.7,33.8)	41 (24,78.15)	51.4 (26.15,93.8)	20.638,<0.001	0.002, <0.001, 1.000
AST (U/L)	21.05 (17.45,30.4)	35.1 (25.8,57.65)	47(27.9,75.5)	32.769,<0.001	0.001, 0.001, 0.823
TBIL(μmol/L)	13.98±4.31	15.2±4.69	13.81±4.31	1.249,0.29	0.413,0.981,0.318
GGT (U/L)	31.3(20.25,47)	46(30.89,63.9)	57(34.05,70.9)	16.959,<0.001	0.019, <0.001, 0.586
ALP ((U/L)	78.18±20.77	77.86±18.86	87.66±25.67	2.777,0.066	0.998,0.113, 0.1
TC (mmol/L)	4.72±0.95	4.79±0.83	5.65±1.0	13.584,<0.001	0.938, 0.001, <0.001
TG (mmol/L)	1.57(1.41,2.5)	1.76(1.41,2.78)	2.88(1.84,4.02)	12.863,0.002	1.000, 0.002, 0.025
HDL-C (mmol/L)	1.15±0.23	1.03±0.19	0.98±0.26	6.165,0.003	0.035,0.003,0.672
LDL-C (mmol/L)	2.34±0.69	2.66±0.72	3.32±0.8	19.622,<0.001	0.119, <0.001, <0.001
VLDL-C (mmol/L)	0.99 (0.73, 1.35)	1.34(0.83,1.78)	1.45(1.22,2.11)	15.455,<0.001	0.130, <0.001, 0.173
ApoA1 (g/L)	1.28±0.25	1.31±0.22	1.3±0.29	0.116,0.89	0.892, 0.929, 0.996
ApoB (g/L)	0.97±0.19	1.01±0.22	1.2±0.26	13.273,<0.001	0.608, <0.001, <0.001

Variable	GSDMD tertile 1 (n=44)	GSDMD tertile 2 (n=43)	GSDMD tertile 3 (n=43)	Statistical value, p	p1, p2, p3
UA(μmol/L)	332.41±86.29	358.1±93.84	376.12±96.59	2.466,0.089	0.399,0.074,0.638
FBG (mmol/L)	7.84±1.76	8.2±1.83	8.3±1.8	0.793,0.455	0.621,0.457,0.963
FINS (uU/ml)	12.51 (7.27,22)	14.23 (9.55,21.6)	14.1 (8.51,23.57)	0.465,0.793	NS, NS, NS
CRP (mg/L)	2.16 (1.48,3.45)	3.26 (1.89,4.26)	4.32 (2.3,5.38)	11.25,0.004	0.857,0.003,0.081

Data are presented as mean ± SD, median (IQR), or n (%), as appropriate. The overall statistical test and P value are shown together in the "Statistical value, P" column; p1, p2, and p3 denote pairwise-comparison P values. GSDMD, gasdermin D.

Figure 3. Correlations of FAST with clinical and pyroptosis-related markers. The heatmap displays correlation coefficients between FAST and clinical, metabolic, liver-related, and pyroptosis-related variables. The color scale indicates the direction and magnitude of the correlation coefficients. FAST, FibroScan-AST score; GSDMD, gasdermin D; IL-1β, interleukin-1β.

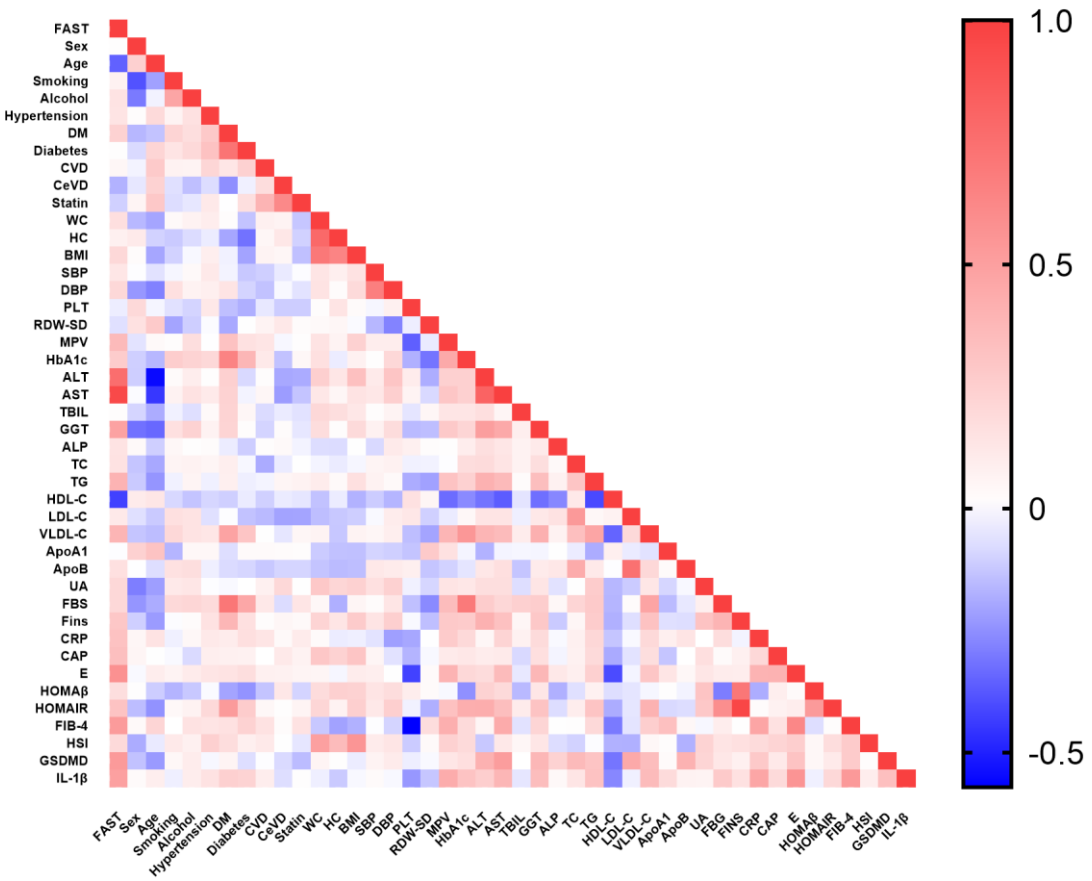


Table 3. Correlations of FAST with clinical and biomarker variables

FAST					
Variable	r	p	Variable	r	p

FAST					
FAST	1	-	TBIL	0.001	0.993
Sex	-0.001	0.993	GGT	0.471	＜0.001
Age	-0.353	＜0.001	ALP	0.147	0.096
Smoking	0.071	0.425	TC	0.148	0.094
Alcohol	0.122	0.167	TG	0.38	＜0.001
Hypertension	0.133	0.13	HDL-C	-0.418	＜0.001
DM	0.216	0.014	LDL-C	0.108	0.221
CVD	0.044	0.617	VLDL-C	0.384	<0.001
CeVD	-0.176	0.045	ApoA1	-0.009	0.919
Statin	-0.113	0.199	ApoB	0.16	0.07
WC	0.163	0.063	UA	0.182	0.038
HC	0.07	0.426	FBG	0.176	0.045
BMI	0.203	0.021	FINS	0.286	0.001
SBP	0.114	0.198	CRP	0.302	＜0.001
DBP	0.196	0.026	CAP	0.324	＜0.001
PLT	-0.016	0.855	LSM	0.544	＜0.001
RDW-SD	-0.059	0.508	HOMA-β	0.184	0.037
MPV	0.338	＜0.001	HOMA-IR	0.296	0.001
HbA1c	0.242	0.006	FIB-4	0.515	＜0.001
ALT	0.759	＜0.001	HSI	0.201	0.022
AST	0.95	＜0.001	GSDMD	0.503	＜0.001
IL-1β	0.468	＜0.001			

Correlation coefficients (r) and two-sided P values are shown. FAST, FibroScan-AST score; GSDMD, gasdermin D; IL-1β, interleukin-1β.

Table 4. Univariable logistic regression for FAST-defined high-risk MASH

Variables	β	SE	Wald χ^2	P-value	OR	95% CI for OR
Age	-0.078	0.024	10.439	0.001	0.925	0.882–0.970
DM	1.364	0.478	8.144	0.004	3.911	1.533–9.979
WC	0.033	0.016	4.044	0.044	1.034	1.001–1.067
BMI	0.115	0.056	4.244	0.039	1.122	1.006–1.252
MPV	0.555	0.16	12.084	0.001	1.742	1.274–2.382
HbA1c	0.295	0.098	9.024	0.003	1.344	1.108–1.629
ALT	0.078	0.015	27.207	<0.001	1.081	1.050–1.114
AST	0.317	0.069	21.118	<0.001	1.373	1.200–1.572
GGT	0.043	0.01	18.934	<0.001	1.044	1.024–1.064
TG	0.456	0.146	9.747	0.002	1.578	1.185–2.101
HDL-C	-2.357	0.819	8.29	0.004	0.095	0.019–0.471
VLDL-C	0.895	0.276	10.527	0.001	2.447	1.425–4.200
FBG	0.219	0.103	4.517	0.034	1.245	1.017–1.524

Variables	β	SE	Wald χ^2	P-value	OR	95% CI for OR
FINS	0.035	0.017	4.441	0.035	1.036	1.002–1.070
CRP	0.27	0.095	8.065	0.005	1.31	1.087–1.579
CAP	0.021	0.007	9.989	0.002	1.021	1.008–1.035
LSM	0.806	0.162	24.864	<0.001	2.24	1.631–3.075
HOMA-IR	0.081	0.039	4.276	0.039	1.084	1.004–1.171
FIB-4	2.068	0.46	20.195	<0.001	7.906	3.209–19.481
HSI	0.101	0.045	5.082	0.024	1.106	1.013–1.208
GSDMD	0.04	0.008	23.902	<0.001	1.041	1.024–1.057
IL-1β	0.3	0.07	18.486	<0.001	1.35	1.177–1.547

β, regression coefficient; SE, standard error; OR, odds ratio; CI, confidence interval; FAST, FibroScan-AST score; MASH, metabolic dysfunction-associated steatohepatitis.

Table 5. Multicollinearity diagnostics for multivariable model variables

Variables	VIF	1/VIF
Age	1.843	0.543
BMI	1.154	0.867
HbA1c	1.143	0.875
TG	1.168	0.856
FIB-4	1.511	0.662
IL-1β	1.619	0.618
GSDMD	1.082	0.924

VIF, variance inflation factor. Values >5 were considered indicative of substantial multicollinearity.

Table 6. Sequential multivariable models for FAST-defined high-risk MASH

Variables	Model 1 OR (95%CI)	P	Model 2 OR (95%CI)	P	Model 3 OR (95%CI)	P	Model 4 OR (95%CI)	P
Age	0.945 (0.898–0.994)	0.028	0.862 (0.800–0.928)	<0.001	0.824 (0.753–0.902)	<0.001	0.839 (0.764–0.920)	<0.001
BMI	1.065 (0.945–1.200)	0.303	1.194 (1.025–1.390)	0.023	1.201 (1.018–1.416)	0.03	1.238 (1.036–1.480)	0.019
HbA1c	1.260 (1.030–1.542)	0.025	1.207 (0.933–1.561)	0.153	1.068 (0.813–1.403)	0.638	1.112 (0.832–1.487)	0.474
TG	1.401 (1.034–1.896)	0.029	1.118 (0.781–1.601)	0.543	0.908 (0.606–1.360)	0.639	0.903 (0.605–1.349)	0.619

Variables	Model 1 OR (95%CI)	P	Model 2 OR (95%CI)	P	Model 3 OR (95%CI)	P	Model 4 OR (95%CI)	P
FIB-4	—	—	24.499 (6.658–90.151)	<0.001	16.594 (4.549–60.528)	<0.001	16.560 (4.170–65.771)	<0.001
IL-1β	—	—	—	—	1.372 (1.091–1.727)	0.007	1.303 (1.018–1.668)	0.036
GSDMD	—	—	—	—	—	—	1.032 (1.010–1.055)	0.004

Model 1 included age, BMI, HbA1c, and TG; Model 2 added FIB-4; Model 3 added IL-1β to Model 2; and Model 4 added GSDMD to Model 3. ORs are presented with 95% CIs. BMI, body mass index; CI, confidence interval; FIB-4, fibrosis-4 index; GSDMD, gasdermin D; HbA1c, glycated hemoglobin; IL-1β, interleukin-1β; OR, odds ratio; TG, triglycerides.

Table 7. Discrimination of individual and combined biomarkers

Marker	AUC (95% CI)	Cutoff	Sensitivity	Specificity	PPV	NPV	Youden index
FIB-4	0.768 (0.685-0.85)	≥1.3345	66.70%	79.10%	75.00%	71.60%	0.458
GSDMD	0.785 (0.702-0.867)	≥52.88	85.70%	71.60%	74.00%	84.20%	0.573
IL-1β	0.747 (0.663-0.831)	≥2.1325	73.00%	65.70%	66.70%	72.10%	0.387
FIB4+GSDMD	0.845 (0.78-0.909)	≥0.2552	93.70%	59.70%	68.20%	91%	0.534
FIB4+IL-1β	0.804 (0.729-0.88)	≥0.6518	55.60%	92.50%	87.50%	68.90%	0.481
FIB4+IL-1β+ GSDMD	0.859 (0.798-0.919)	≥0.3668	82.50%	71.60%	73.20%	81.40%	0.541

Optimal cutoffs were selected by maximizing the Youden index. AUC, area under the receiver operating characteristic curve; CI, confidence interval; FIB-4, fibrosis-4 index; GSDMD, gasdermin D; IL-1β, interleukin-1β; NPV, negative predictive value; PPV, positive predictive value.

Figure 4. ROC curves of individual and combined biomarkers for high-risk MASH. Receiver operating characteristic curves compare FIB-4, GSDMD, IL-1β, and combined biomarker models for discriminating FAST-defined high-risk MASH. AUC values and 95% confidence intervals are shown in the figure key. AUC, area under the receiver operating characteristic curve; FIB-4, fibrosis-4 index; GSDMD, gasdermin D; IL-1β, interleukin-1β; FAST, FibroScan-AST score; MASH, metabolic dysfunction-associated steatohepatitis.

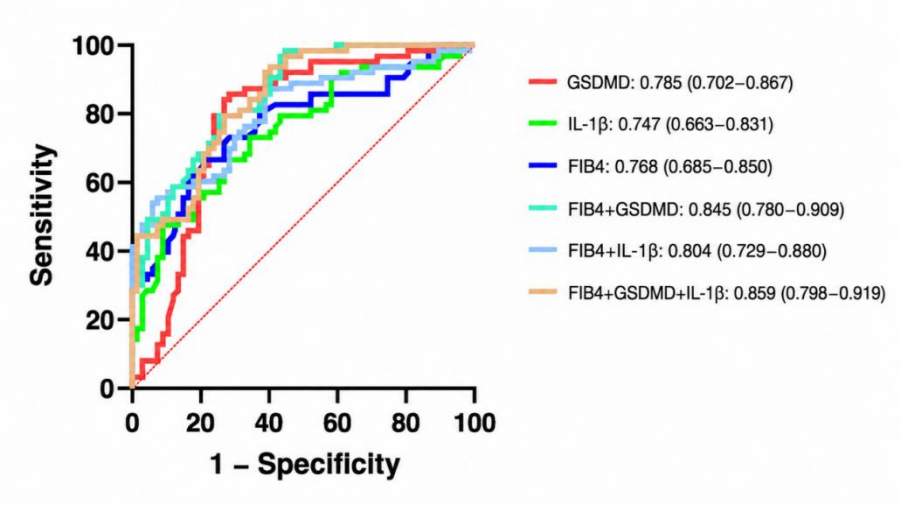


Table 8. DeLong comparisons of sequential multivariable model AUCs

Model	Predictors	AUC (95% CI)	ΔAUC (95% CI)	DeLong P value
Model 1	Clinical factors	0.746 (0.661–0.831)	Reference	-
Model 2	Model 1 + FIB-4	0.889 (0.837–0.942)	0.143 (0.070–0.217)	<0.001
Model 3	Model 2 + GSDMD	0.913 (0.866–0.959)	0.167 (0.090–0.243)	<0.001
Model 4	Model 2 + IL-β	0.905 (0.856–0.953)	0.158 (0.080–0.237)	<0.001
Model 5	Model 2 + IL-β + GSDMD	0.916 (0.870–0.961)	0.170 (0.092–0.248)	<0.001

Model 1 included age, BMI, HbA1c, and TG; Model 2 added FIB-4; Model 3 added GSDMD to Model 2; Model 4 added IL-1β to Model 2; and Model 5 added both GSDMD and IL-1β to Model 2. ΔAUC is the change in AUC relative to Model 1. DeLong tests compare each extended model with Model 1. AUC, area under the receiver operating characteristic curve; BMI, body mass index; CI, confidence interval; FIB-4, fibrosis-4 index; GSDMD, gasdermin D; HbA1c, glycated hemoglobin; IL-1β, interleukin-1β; TG, triglycerides.

Figure 5. ROC curves of multivariable models for high-risk MASH. Receiver operating characteristic curves compare Models 1–5 for discriminating FAST-defined high-risk MASH. Model 1 included age, BMI, HbA1c, and TG; Model 2 added FIB-4; Model 3 added GSDMD to Model 2; Model 4 added IL-1β to Model 2; and Model 5 added both GSDMD and IL-1β to Model 2. AUC values and 95% confidence intervals are shown in the figure key. AUC, area under the receiver operating characteristic curve; BMI, body mass index; FIB-4, fibrosis-4 index; GSDMD, gasdermin D; HbA1c, glycated hemoglobin; IL-1β, interleukin-1β; TG, triglycerides.

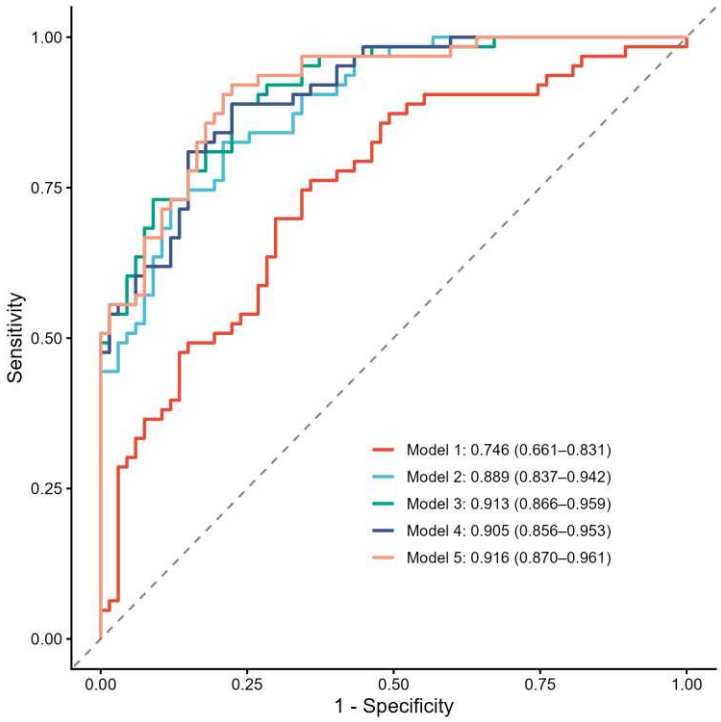


Table 9. NRI and IDI for sequential multivariable models

Model	AUC (95% CI)	P value (AUC)	NRI (95% CI)	P value (NRI)	IDI (95% CI)	P value (IDI)
Model 1	0.746 (0.661–0.831)	-	-	-	-	-
Model 2	0.889 (0.837–0.942)	0	1.0685 (0.7806–1.3563)	<0.001	0.2687 (0.1891–0.3483)	<0.001
Model 3	0.913 (0.866–0.959)	0	1.1376 (0.8547–1.4206)	<0.001	0.3369 (0.2531–0.4207)	<0.001
Model 4	0.905 (0.856–0.953)	0	1.1618 (0.884–1.4396)	<0.001	0.3114 (0.2289–0.394)	<0.001
Model 5	0.916 (0.870–0.961)	0	1.2926 (1.0301–1.555)	<0.001	0.3622 (0.278–0.4465)	<0.001

Models 2–5 were compared with Model 1. AUC, area under the receiver operating characteristic curve; CI, confidence interval; IDI, integrated discrimination improvement; NRI, net reclassification improvement.

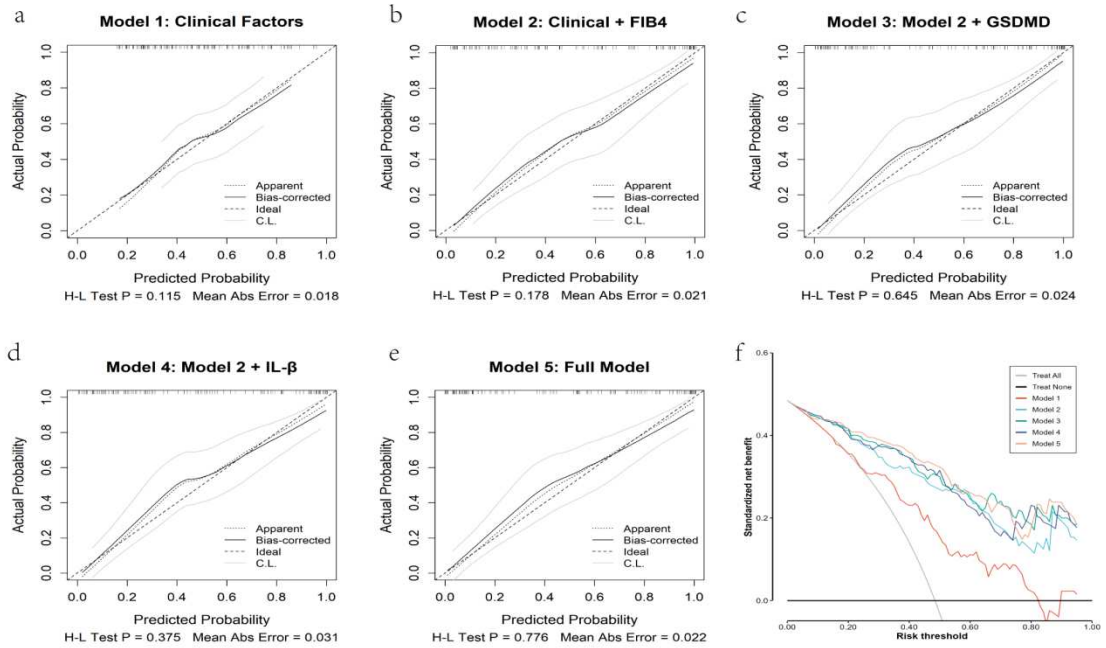
Table 10. Calibration metrics for multivariable models

Model	Brier score	Calibration intercept	Calibration slope	H-L test P value
Model 1	0.204	-0.007	0.866	0.115

Model	Brier score	Calibration intercept	Calibration slope	H-L test P value
Model 2	0.139	-0.025	0.865	0.178
Model 3	0.122	-0.028	0.825	0.645
Model 4	0.129	-0.023	0.85	0.375
Model 5	0.115	-0.038	0.799	0.776

665 Calibration was assessed using 1,000 bootstrap resamples. H-L, Hosmer–Lemeshow.

666 **Figure 6.** Calibration and decision curve analyses of multivariable models.



667

668 (a–e) Calibration curves for Models 1–5, showing apparent and bias-corrected estimates against the ideal
669 reference line. (f) Decision curve analysis showing net clinical benefit across threshold probabilities; "treat all"
670 and "treat none" are shown for reference. Model 1 included age, BMI, HbA1c, and TG; Model 2 added FIB-4;
671 Model 3 added GSDMD to Model 2; Model 4 added IL-1β to Model 2; and Model 5 added both GSDMD and
672 IL-1β to Model 2. BMI, body mass index; DCA, decision curve analysis; FIB-4, fibrosis-4 index; GSDMD,
673 gasdermin D; HbA1c, glycated hemoglobin; IL-1β, interleukin-1β; TG, triglycerides.

674 # List of abbreviations

Abbreviation	Full term
MASLD	Metabolic dysfunction-associated steatotic liver disease
WC	Waist circumference
HC	Hip circumference
BMI	Body mass index
SBP	Systolic blood pressure
DBP	Diastolic blood pressure

Abbreviation	Full term
PLT	Platelet count
RDW-SD	Red blood cell distribution width-standard deviation
MPV	Mean platelet volume
HbA1c	Glycated hemoglobin
ALT	Alanine aminotransferase
AST	Aspartate aminotransferase
TBIL	Total bilirubin
GGT	Gamma-glutamyl transferase
ALP	Alkaline phosphatase
TC	Total cholesterol
TG	Triglycerides
HDL-C	High-density lipoprotein cholesterol
LDL-C	Low-density lipoprotein cholesterol
VLDL-C	Very-low-density lipoprotein cholesterol
ApoA1	Apolipoprotein A1
ApoB	Apolipoprotein B
UA	Uric acid
FBG	Fasting blood glucose
FINS	Fasting insulin
CRP	C-reactive protein
GSDMD	Gasdermin D
IL-1β	Interleukin-1β
CAP	Controlled attenuation parameter
LSM	Liver stiffness measurement
HOMA-β	Homeostasis model assessment of β-cell function
HOMA-IR	Homeostasis model assessment of insulin resistance
FIB-4	Fibrosis-4 index
HSI	Hepatic steatosis index
FAST	FibroScan-AST score